TIME-OF-PROPAGATION COUNTER — A NEW CHERENKOV RING IMAGING DETECTOR —

Takayoshi Ohshima*
Physics Department, Nagoya University
Chikusa, Furo, Nagoya 464-8602, Japan

ABSTRACT

A new particle identification detector based on measurements of both Time-of-Propagation (TOP) and horizontal emission angle (Φ) of Cherenkov photons is proposed here. Some R&D results are also reported.

1 Introduction

Measuring of the Cherenkov angle ($\theta_{\rm C}$) is currently one of the most promising way to identify high-energy charged particles. Depending on the particle, its momentum range, and experimental condition, there are a various ways to do this using liquid, gas, or solid radiators with gas chambers or photo-multiplier tubes (PMT) as photon detectors. The Cherenkov ring image can be created using the proximity focussing, focussing mirrors, or pin hole projection, such as in RICH[1] and DIRC[2] type of devices. We propose here a new approach to the DIRC method, by measuring the ring image detecting both Time-Of-Propagation (TOP) of Cherenkov photons in the quartz radiator bar and horizontal emission angle (Φ) at the bar-end. This is in contrast to the BaBar DIRC, which measures the x and y coordinates.

In order to further improve the particle identification (PID) ability of the KEKB-BELLE spectrometer[3], in particular the K/π separation, the new detector should be compact in radial direction. The first attempt to propose a compact DIRC detector was a focussing counter, proposed by Kamae et al.[4]. It would eliminate a large projection volume, such as in the BABAR DIRC[2]. A small, vertically focussing mirror was proposed to reduce the vertical aberration. However, the horizontal aberration still remained, thereby weakening the PID ability of such a device, especially in the case of inclined incident particles. The proposed TOP counter, which uses the horizontal focussing, renders both of these aberrations effectively harmless. In addition, it can be made compact, and deliver the good particle separation.

To aid the readers in visualizing the principle of TOP counter, Fig. 1 illustrates the internaly reflecting Cherenkov photons propagating in a rectangular quartz bar: (a) top view and (b) side view. TOP is inversely proportional to the z-component of the light velocity: TOP(ns) = 4.90 $\times L$(m) / $q_{\rm z}$, where $q_{\rm z}$ is the z-component of unit velocity vector and L is the propagation length along z direction. Let's briefly evaluate separation ability using this method. For example, the TOP difference between 4 GeV/c K and π is about 100 ps or larger for L = 2 m. Therefore, a

*Author's e-mail: ohshima@hepl.phys.nagoya-u.ac.jp, tel: +81-52-789-2447, telefax: +81-52-782-5752.

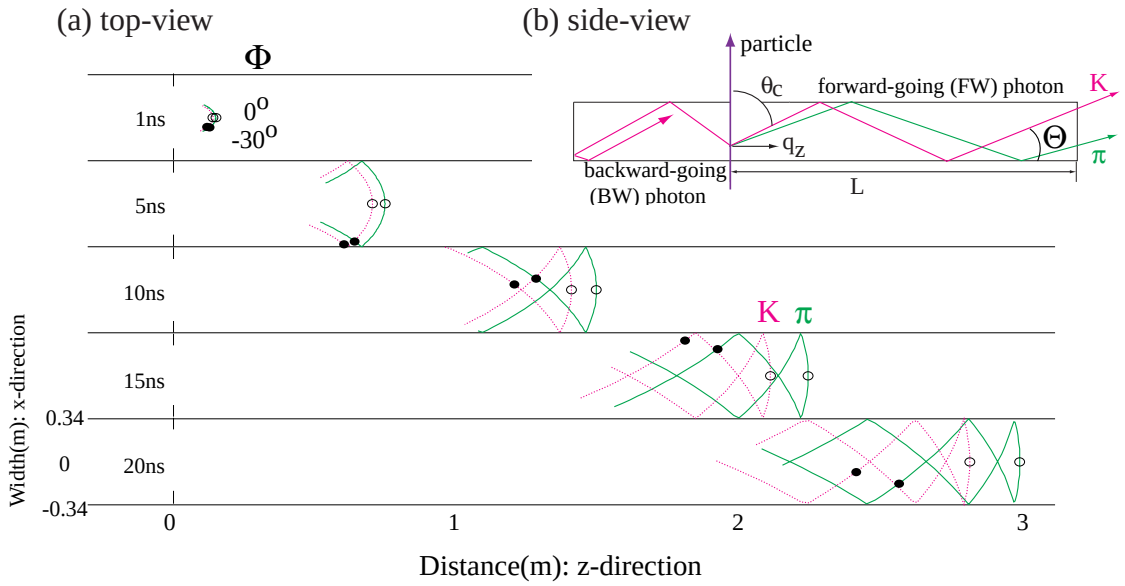

Figure 1: Illustration of PID principle of TOP counter. Parts of Cherenkov ring image, produced by a charged K and π with a normal incident onto this plane, are shown as propagating in a quartz-bar in (a). The quartz-bar has a rectangle cross section, width of which is set to 0.68 m for an illustration purpose, and its refractive index is $n = 1.47$. The elapsed time in ns is shown at the left-hand side. Curves (every 1° step in Φ) are the Cherenkov rings for π and K, respectively, and open and closed circles indicate photons emitted at $\Phi = 0°$ and $-30°$. A side view of propagating photons is illustrated in (b). The photo-multipliers are placed in such a way as to detect the reflected photons (BW) toward the detectors (see also Figure 2). TOP is inversely proportional to the z-component of unit velocity vector (q_z).

time measurement with $\sigma = 100$ ps for a single photon yields 1 σ separation, and accordingly the total separation gives approximately a square-root of detectable number of photons (N_{ph}) times σ. That is, forward-going (FW) detectable photons is $N_{ph} \approx 30$ for a normal incident particle to 20 mm-thick quartz radiator, and its separation is expected to be 5.5 σ. When the backward-going (BW) photons are also detected as illustrated in Fig.1(b) by reflecting at an opposite end, the separation could be enhanced further by a factor of $\sqrt{2}$.

The TOP counter is a Time-Of-Flight counter, which detects the Cherenkov photons rather than the scintillation photons. Two substantial and undesirable effects of the precise TOF counters with the plastic scintillators can be eliminated: 1) While a decay-constant of fast counting scintillator is typically ~2 ns, the Cherenkov radiation does not have a decay mechanism, so no corresponding effect exists. 2) While the propagation paths of scintillation photons to a certain horizontal emission angle Φ, (see Fig. 1(a)) are not unique due to their uniform emission over 4π solid angle, they are unique for the Cherenkov radiation photons. Because of this, the Cherenkov photons could provide a comparable or even higher time resolution than the TOF scintillation counter, in spite of having fewer radiated photons. The Cherenkov Correlated Timing detector [5] is similar to the TOP counter, but without the Φ angle segmentation.

In order to evaluate the achievable K/π separability of the TOP counter, we optimize its parameters as illustrated in Fig. 2, where the butterfly-shaped horizontal focussing mirror with an arc radius of 250 mm is designed to have the

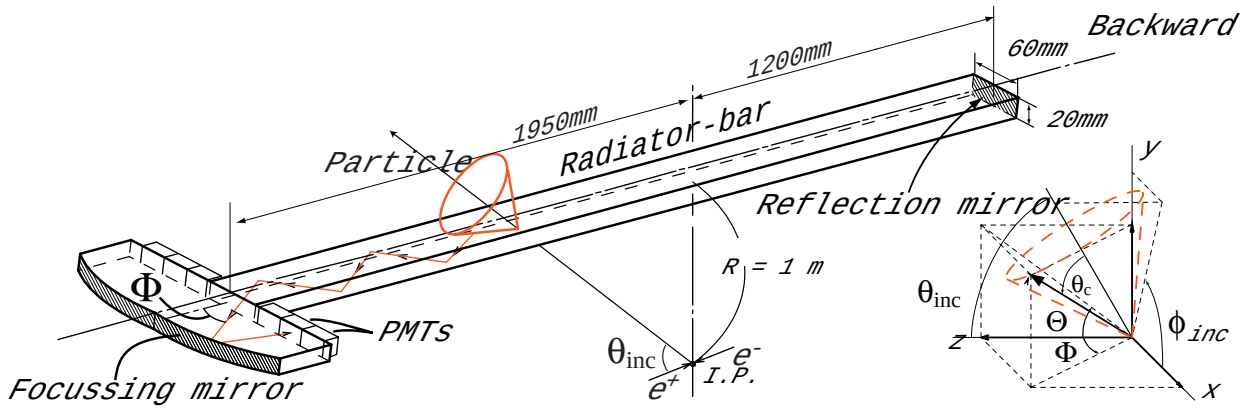

Figure 2: Structure of the TOP counter. Basic parameters are indicated in the figure. Anode array of PMTs is arranged on the focal line of the butterfly-shaped focussing mirrors along to x direction. Since KEKB is an asymmetric collider, the quartz-bar is accordingly configured as z-asymmetric relative to the interaction point (IP).

Φ-aparture of $\pm 45^o$ and dispersion of $d\Phi/dx = 0.5^o/1$ mm. Root-mean-square of the focussed accuracy is $\Delta x \approx \pm$ 0.4 mm. The radiator-bar has a length of 3150 mm, width of 60 mm and thickness of 20 mm, and its backward-end surface has a reflecting mirror. The bar and focussing mirrors are made out of synthetic optical quartz with refractive index (n) of 1.47 at wavelength of $\lambda = 390$ nm. These counters would be placed at 1 m radially away from the interaction point of the KEKB-BELLE detector to form a cylindrical structure as the barrel PID counter.

The differences of TOP and TOF (measured from IP to the TOP counter) between K and π have the same sign under most conditions, and therefore adding both TOF and TOP could improve the separation; therefore, TOP is hereafter defined as a sum of TOP and TOF, unless otherwise specified.

2 Expected Separability

There are three dominant contributions which limit the best possible K/π separability:

(1) chromatic effect of the Cherenkov photons,

(2) aberration effect of the focussing mirror, and

(3) transit time spread (TTS) of the photomultiplier tube (PMT).

Figure 3 shows TOP errors from the above three contributions, and the K/π TOP and TOP+TOF time differences, δ(TOP) and δ(TOP + TOF), for two examples representing the BELLE experimental conditions (see also Ref.[6], which discusses other cases). Since both contributions,(1) and (2), rise steeply at large Φ, Φ acceptance is limited to $|\ \Phi\ | < 45^o$. Adding the error in the TTS, $\sigma_{\rm TTS} = 80$ ps, which will be discussed later, and other contributions, such as the start-signal uncertainty of 25 ps, results in a total uncertainty of 84 ps for error (3). When a particle's incident polar angle $\theta_{\rm inc}$ gets smaller than 40^o, δ(TOP) reverses its sign compared to the TOF difference (see Fig. 3(b)), and the separation power decreases somewhat.

The expected detectable number of FW photons is approximately 35 and 115, for examples shown in Fig. 3(a) and 3(b), respectively, assuming the PMT's quantum efficiency (QE) of $\approx$25%. When the particle hits the TOP counter at $\theta_{\rm inc} \sim 90^o$, it also exits a sufficient number of BW photons. They reach PMT's 15-20 ns later compared

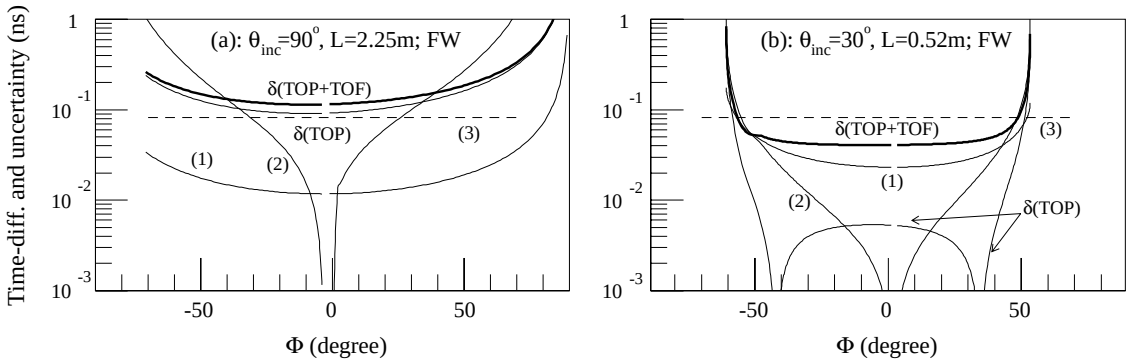

Figure 3: Three dominant contributions to time measurement error, (1), (2) and (3), as discussed in text, and TOP differences for 4 GeV/c K and π. TOP counter (see Fig.2) is configured to form a cylindrical shape and operates at B=1.5 T in KEKB-BELLE. $\theta_{\rm inc}$ is the polar angle of an emitted particle from IP (see Fig.2). In these figures, only FW photons are taken into consideration. In (b) δ(TOP) has negative sign at $\mid \Phi \mid < 40^{\rm o}$. Due to the magnetic field effect, the incident particle to the TOP counter is bent in the azimuthal direction and therefore the contributions are not symmetric, as seen in figures.

to FW photons, and therefore the detection and the identification of both FW and BW photons is relatively easy. When the particle hits the TOP counter at $\theta_{\rm inc} > 90^{\rm o}$, the BW photons play the leading role.

Before examining the expected separability, we would like to bring attention to some specific aspects of the TOP counter.

- The time spread of Cherenkov radiation along the particle trajectory over the thickness of quartz bar is compensated by the corresponding variation of photon propagation time. The maximum variation of the sum of these times, which is σ ~20 ps, occurs at the normal incidence, and it is less than 20 ps at any other incident angle. This effect is much smaller than PMT's TTS, and therefore the vertical aberration is negligible for the TOP measurement.
- Figure 4(a) and 4(b) show (TOP+TOF) distributions as a function of Φ for the horizontal focussing, and as a function of the vertical emission angle Θ for the vertical focussing, respectively. In the former case, the photons distribute rather uniformly over the angle, and also the slope ∂(TOP + TOF)/∂(angle) is rather smaller compared to the second case.. Therefore the horizontal focussing was chosen to achieve a better resolution and also easier detection.
- The contribution from the multiple scattering (MS) is also small: $\Delta\theta^{\rm rms}_{\rm space}$(MS) is 2.9, 1.5, 0.98, and 0.74 mrad, while the difference of K/π Cherenkov angles $\Delta\theta_{\rm C;K/\pi}$ is 104, 25.9, 11.6, and 6.5 mrad for a normal incident 1, 2, 3, and 4 GeV/c particle, respectively.
- The BELLE-CDC (Central Drift Chamber) provides precise enough information, regarding the particle incident position, angle and momentum, to nullify their effects on the TOP measurement. The z-position resolution is about 2 mm, which corresponds to a time uncertainty of about 10 ps. Ambiguity of momentum measurement leads to an uncertainty of the Cherenkov emission angle, as $\sigma_{\theta_{\rm C}} = \left(\frac{\cot\theta_{\rm C}}{\gamma^2}\right) \cdot \left(\frac{\sigma_{\rm p}}{p}\right)$: This uncertainty is much smaller than $\Delta\theta_{\rm C;K/\pi}$ even at $\sigma_{\rm P}$/p = 1 %. The error in the particle's incident angle $\theta_{\rm inc}$, contributes less than 10 ps in error of the TOP measurement , in the case of BELLE, because $\phi_{\rm inc}$ error does not intrinsically affect TOP since $\frac{\partial q_z}{\partial \phi_{\rm inc}} \mid_{\theta_{\rm inc}} = 0$.

Taking into account all contributions mentioned above, a simulation study assumed to measure only the eariest arrival photon at individual anodes, and assuming that PMTs have $\sigma_{\rm TTS}$ = 80 ps and anode width of 1 mm. A reference (TOP vs Φ)- distributions are obtained for Cherenkov photons generated at the middle of quartz thickness, with n = 1.47 and by K and π particles.

Figure 4 shows results of these simulations (open circles and crosses), including the reference distributions (curves). Figure 5 shows the Log-Likelihood distribution, includeing the reference. The resulting separability is $\mathcal{S}(=\sqrt{2\Delta ln\mathcal{L}})$ = 5.7 for 4 GeV/c K/π at $\theta_{\rm inc}$ = 90°. Figure 6 shows the calculated separabilities of the TOP counter for the BELLE configuration. Figure 6 also shows the separability for π's in $B \to \pi\pi$ decay (a thick curve), which represents the highest momentum limit at the BELLE experiment. It is found that $\mathcal{S}$ >5 could be achieved at any barrel region of $\theta_{\rm inc}$ = 30° - 130°.

3 Multi-anode PMTs

We are performing R&D on two kinds of PMTs for the TOP counter. The photon detector should have the following properties:

- Single photon sensitivity,
- High time resolution, for example, $\sigma_{\rm TTS} \leq 100$ ps,
- Position sensitivity, for example, $\sigma_{\rm x} < 0.5$ mm,
- Operability under magnetic field of 1.5 T at BELLE.

The first three items are well realized by a commercially available PMT: Hamamatsu R5900U-00-L16. Our R&D work on the TOP counter is proceeding with this PMT, as reported below. L16 is a linear-array 16-anode PMT with 0.8×16 mm^2 anodes of 30×30 mm^2 size and 1 mm pitch. It has a gain of 2×10^6 at a supply voltage of 800 V over 10 dynodes, and gives a 0.6 ns risetime. We adjusted the HV divider to supply higher voltage to the first two dynodes, compared to a standard design, in order to reach the time resolution of σ <100 ps. Figure 7 shows the measured time resolutions in the single photon mode, as a function of (a) the ADC pulse-height using all 16 channels of the L16 PMT, and (b) the anode number withing the L16 PMT (about 75 ps was obtained on average). The data were obtained using a 400 nm light pulser, and with a 1 mm-wide slit in front of the PMT. Without the slit, cross-talk was observed, especially under a high multi-photon irradiation, which also affected the resolution. Its study is being carried out now.

Since L16 cannot operate in a large magnetic field, we have been examining other possibility, such as the fine-mesh multi-anode PMTs: Hamamatsu R6135MOD-L24 (square shaped of area 39×39 mm^2) and L24X (round shaped). L24 has 24 anodes of size 0.8×26.5 mm^2, and pitch of 1.1 mm. While L24 has a 2.5 mm distance between the photocathode and the first dynode, L24X has 1 mm distance, but keeping other essential parameters the same. With 24 dynodes, a gain of $2(8)\times10^7$ is achieved at 1500 (2000) volts for L24 (L24X). With no magnetic field, the position resolution is only about 2 mm, however, for field higher than 0.2 T, it improves to σ <0.5 mm, as seen in Fig. 8(a). The fine-mesh type PMT does not yield a peak in the single photon distribution spectrum, but instead a continuous distribution without a deep valley between signal and noise, as indicated in Fig. 8(b). Time resolution is measured, for L24X, by varying the magnetic field strength under which the maximum allowed high-voltages are applied. This data are plotted in Fig. 8(c) as a function of gain relative to that with no magnetic field. The PMT's gain reduces quickly with the magnetic field and time resolution also gets worse. To date we have reached σ ∼120 ps at B <0.6 T.

4 Beam Test

In order to confirm the essential and expected characteristics of the TOP counter, beam tests were performed at KEK-PS using π beam. A test counter was constructed with the structure as described in Fig. 2, but the quartz bar length was 1 m and an absorptive filter instead of the reflection mirror for BW photons at the bar end was prepared. Six L16 PMTs were attached to the focussing mirrors and accordingly, 96 anode signals in total were read out. Overall detection efficiency of photons, which come to the focal line surface, not including the PMT's QE, was nearly 20% at current configuration: Photoelectron detection efficiency of the L16 PMT was about 1/2, and an effective coverage by L16 sensitive area over the mirror surface was about 40%. The above PMT's insensitive area, most of which was due to the mechanical structure, would reflect back the photons and such photons hit wrong anodes after being reflected by the aluminum coated focussing mirror (we will call such photons the mirror-reflected photons). In order to avoid this unwanted phenomena, the absorptive filters were inserted in front of such L16 dead surfaces. The time resolution and the mirror-reflected photon distribution were measured by injecting single photons from the light pulser through an upper side of the focussing mirror or the quartz bar.

The beam was tuned to hit the TOP counter at L = 0.02 m nominally. The recorded data are shown in Fig. 9, where a single photon peak is clearly seen in the ADC spectrum, which coincides with the spectrum produced by light pulser single photons. Figure 9(c) shows a timewalk-corrected TDC distribution where two small contributions, besides Cherenkov signal photons, can be found: Cherenkov photons produced by the knock-on electrons, and the mirror-reflected photons. The resulting time resolutions, taking into account all 96 anodes, were about σ = 85 ps, as plotted in Fig. 10. These results are consistent with those observed with the light pulser. The chromatic contribution is insignificant at this configuration, and the L16 PMT's TTS dominates the resolution.

Next, the beam position was moved to L = 1 m, and the beam momentum was set to 1.1, 2, and 4 GeV/c. The expected number of anodes, which fired, was 6, and we observed an average 6.3, at each momentum set. We applied a time cut to reject the contributions from the knock-on electrons and the mirror-reflected photons. Figure 11 shows the observed Cherenkov ring image as a function of Φ angle. Because of longer propagation length in this case, the TDC distribution produced by the knock-on electrons are widely spread. We did not have a beam tracking chamber system, and therefore the beam divergence, as defined by trigger scintillation counters, was not as precise as expected for the BELLE spectrometer, where its contribution is expected to be negligable. Therefore, a simple but tricky analysis was carried out. Triggered samples are required to have a signal in the certain anode. For example, for a case of the 27th anode, a cut within the first 150 ps time duration of its measured raw time distribution of 350 ps (FWHM), would restrict the beam divergence somewhat. Measured resolutions for some anodes are plotted in Fig. 10; a fairly good agreement with the expectation can be seen, allthough one must say that the errors are large. The parabolic rise of the calculated resolution at large Φ is due to the aberration effect of the mirror rather than the chromatic contribution.

5 Discussion and Summary

The TOP counter is compact and has a high particle separability. Due to the horizontal focussing and thin radiator thickness, the size of a quartz bar cross section can be disregarded, and therefore it does not need a large standoff projection space such as with the BaBar DIRC. In order to make this TOP counter feasible, we still need more R&D work.

First, confirmation of basic TOP behavior, especially the performance at L = 1 m or longer distances, and using a tracking chamber during the next beam test.

Second, increasing the detected number of photons is the most important issue, and two approaches are being considered. One way is to employ light-guides between the mirror and the PMTs. Other way is to develop a PMT with larger sensitive area and large number of anodes. Such detector could be utilized, for example, in the fixed target experiment operating with no magnetic field.

To utilize the TOP counter as the next BELLE PID detector, one has to develop a L24 type of PMT, or its equivalent capable of detecting single photons in a large magnetic field of 1.5 T, with position sensitivity of σ_x <0.5 mm and TTS of σ_{TTS} <100 ps. R&D work to develop a L24 type of PMT is under way.

Remarks:

- Adding TOF to TOP helps PID mainly for a low momentum particle. However, for a very long flight-path length, which is possible at some fixed target experiments, one obtains a sufficient separability, as indicated in Table 1, while $\Delta\theta_{C;K/\pi}$ produces only a small TOP difference. Further enhancement of separability can be achieved by improving the PMT's TTS, and/or increasing the detected number of photons. The TOP counter acts in this case as a kind of high resolution TOF counter by means of Cherenkov radiation.

Flight length R(m)	Separability S			
	p = 4 GeV/c		p = 10 GeV/c	
	FW	BW	FW	BW
0	5.7	8.3	1.5	1.5
1	7.4	9.0	1.5	1.5
5	11.7	11.6	1.9	2.2
10	17.6	14.5	3.0	2.9

Table 1: Achievable separabilities with various flight path-length (R). The simulation results of our TOP detector, where FW and BW photons are separately detected, are listed for particles with $\theta_{inc} = 90^\circ$ with no magnetic field. The differences of θ_C between π and K are 6.5 and 1.0 mrad for p = 4 and 10 GeV/c, respectively, and those of the TOF are 231 and 37 ps at R = 10 m.

- Photons propagate in a polished scintillator, keeping their original angle information. It may be interesting to use a scintillator instead of the quartz, although the situation is still not thoroughly understood without an additional investigation. The arrival time distribution of photons at individual Φ segments will spread because of its finite decay time constant and 4π emission. Owing to high TTS making up for a fewer number of photons per segment compared to an ordinary TOF counter, the overall achievable TOF resolution by multi-segment measurements could well be improved.

- Although the separability for particles of large incident angle $\theta_{\rm inc} \leq 120^{\rm o}$ is rather low as seen in Fig. 6, it could be recovered by equipping an inclined reflection mirror, for instance, of $45^{\rm o}$, at the backward end. It makes the reclining Cherenkov ring image stand up to the normal direction so as to propagate the full bar length with the best configuration for separation. While an opposite effect occurs for BW photons generated by a normal incident particle, a rather sufficient TOP difference is already produced by propagating a certain long distance before the photons arrive at the reflection mirror. Optimization of the inclining angle should be investigated.
- The present design of the focussing mirror has a horizontally extended structure that does not seem suitable as a barrel detector. A simple and practical solution is to tilt the counter around the z-axis.

Acknowledgements

I greatly appreciate Mr.Kozaburo Fujimoto for his help to prepare this article in an electronic form. I also gratefully acknowledge Hamamatsu Photonics K. K. for their sincere cooperation to develop L16 and L24 PMTs. This work is supported by Grant-in-Aid for Scientific Research on Priority Area (Physics of CP violation) from the Ministry of Education, Science, and Culture of Japan. The R&D tasks have been carried out by the members of TOP group: M. Akatsu, Y. Enari, K. Fujimoto, Y. Higashino, M. Hirose, T. Hokuue, K. Inami, A. Ishikawa, S. Matsui, T. Matsumoto, K. Misono, T. Ohshima, A. Sugi, A. Sugiyama, S. Suzuki (Nagoya U.), H. Okuno (KEK) and A. Yamaguchi (Tohoku U.).

References

[1] For instance, see, J. Va'vra in Proceedings of 7th Int. Conf. on Instr. for Colliding Beam Physics, INSTR99, Hamamatsu, Japan, November 15-19, 1999.

[2] B. Ratcliff in Proceedings of 7th Int. Conf. on Instr. for Colliding Beam Physics, INSTR99, Hamamatsu, Japan, November 15-19, 1999.

[3] For the description on KEK-B factory and BELLE detector, for instance, see J. Haba, Nucl. Instr. and Methods, A368 (1995) 74; T. Nozaki, Nucl. Phys. B(Proc. Suppl.) 50 (1996) 288.

[4] T. Kamae et al., Nucl. Instr. and Methods A382 (1996) 430.

[5] K. Honscheid, M. Selen and M. Sivertz, Nucl. Instr. and Methods, A343 (1994) 306; H. Kichimi, Nucl. Instr. and Methods, A371 (1996) 87; idib. A371 (1996) 91.

[6] M. Akatsu, M. Aoki, K. Fujimoto, Y. Higashino, M. Hirose, K. Inami, A. Ishikawa, T. Matsumoto, K. Misono, I. Nagai, T. Ohshima, A. Sugi, A. Sugiyama, S. Suzuki, M. Tomoto, and H. Okuno (KEK, Tsukuba), Nucl. Instr. and Methods, A440 (2000) 124-135.

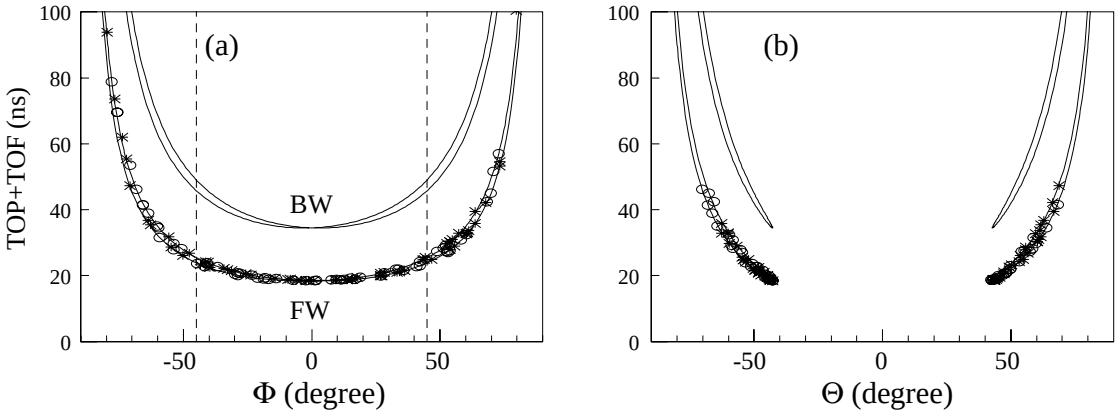

Figure 4: TOP+TOF distributions using (a) horizontal and (b) vertical focussing cases for 4 GeV/c normal incident particle. Because of a tilt in the azimuthal angle of the incident particle due to a magnetic field, two inclined, but symmetric, ring images are formed by FW and BW photons in both cases. Open circles and crosses indicate FW photons generated by π and K particles, respectively, in a simulation study.

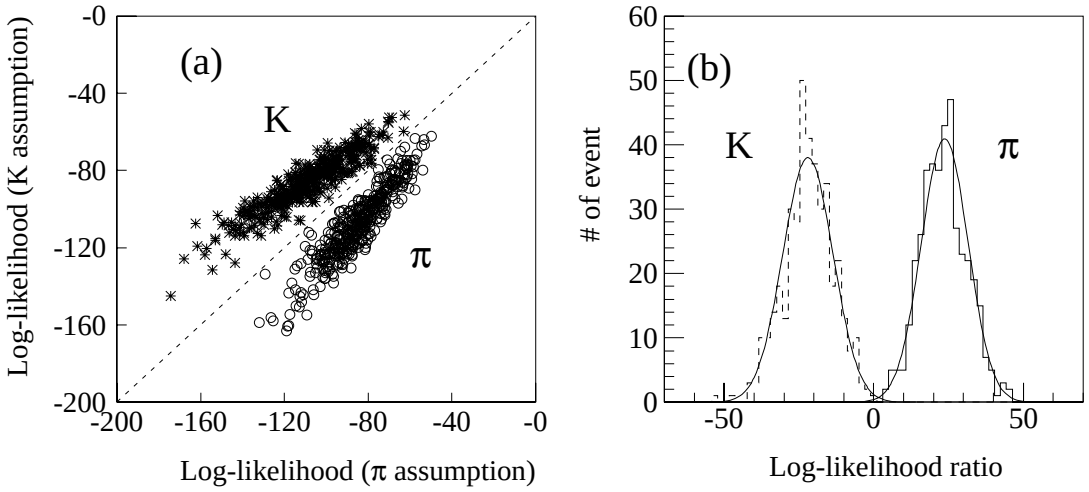

Figure 5: (a) Log-Likelihood distribution for 4 GeV/c K and π at $\theta_{\rm inc} = 90^{\rm o}$. Horizontal and vertical axes indicate the Log-Likelihoods for π and K hypotheses, respectively, and open circles and crosses are the generated π and K samples. (b) The Log-Likelihood ratio distribution.

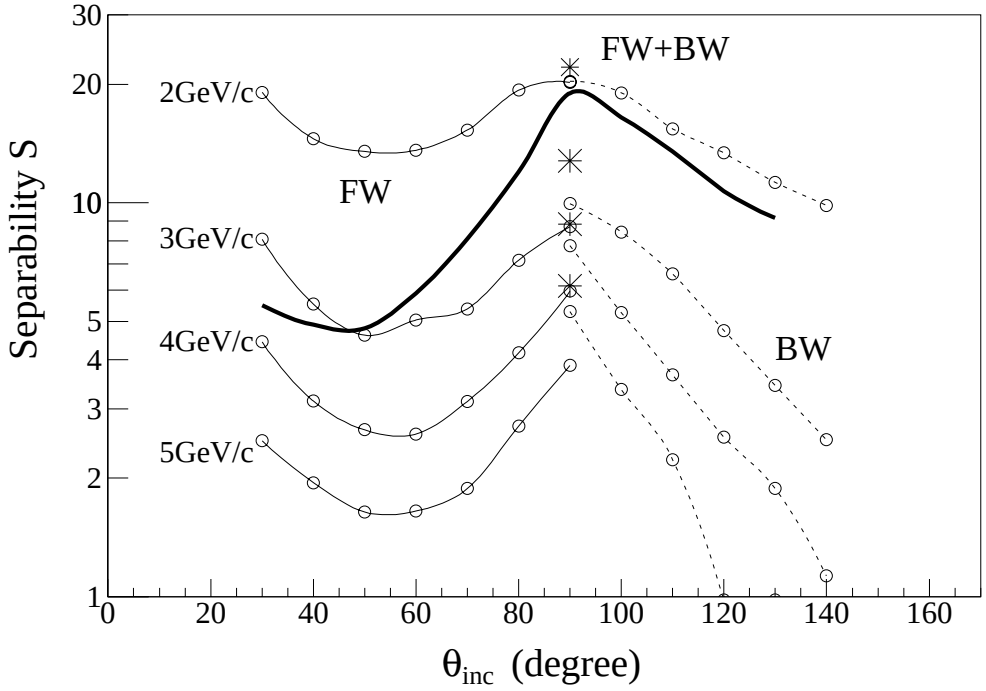

Figure 6: Expected K/π separability for the BELLE configuration. Thin curves are obtained by detecting either FW or BW photons, while crosses are obtained by detecting both photons at $\theta_{\rm inc} = 90^\circ$ case. Momenta of particles are indicated at the left-hand side. The thick curve represents the separability for the highest momentum π's at the BELLE experiment, coming from the decay of $B \to \pi\pi$.

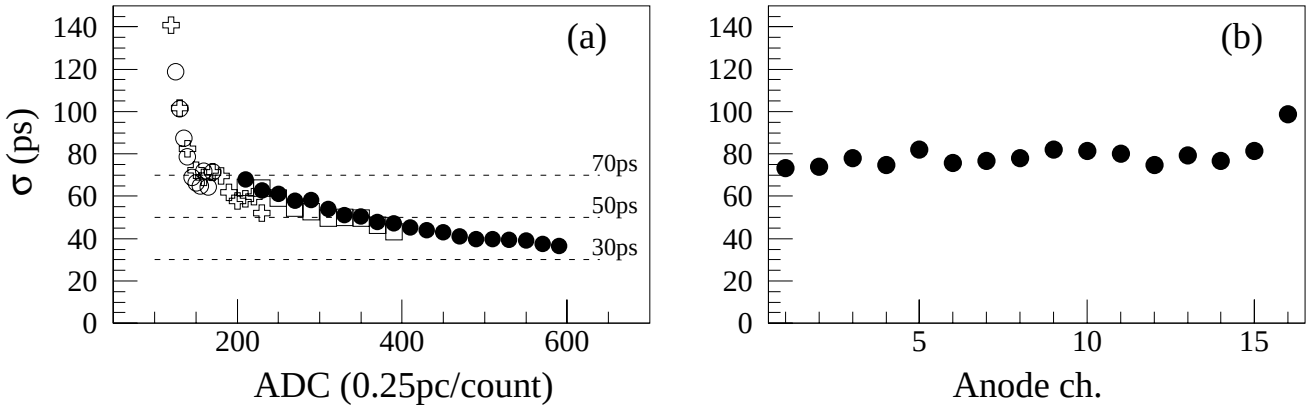

Figure 7: Time resolution of L16 PMT. (a) Time resolution σ vs ADC pulse-height. Measurements were performed four times by changing an intensity of a light pulser, as plotted by open and closed circles, square and crosses. Single photon pulse-height peak corresponds to about 170-th ADC channel. (b) Time resolutions for single photon are measured over all 16 anodes. For (a) and (b), a 1 mm-wide slit is placed in front of the PMT, and HV of 1000 V is applied.

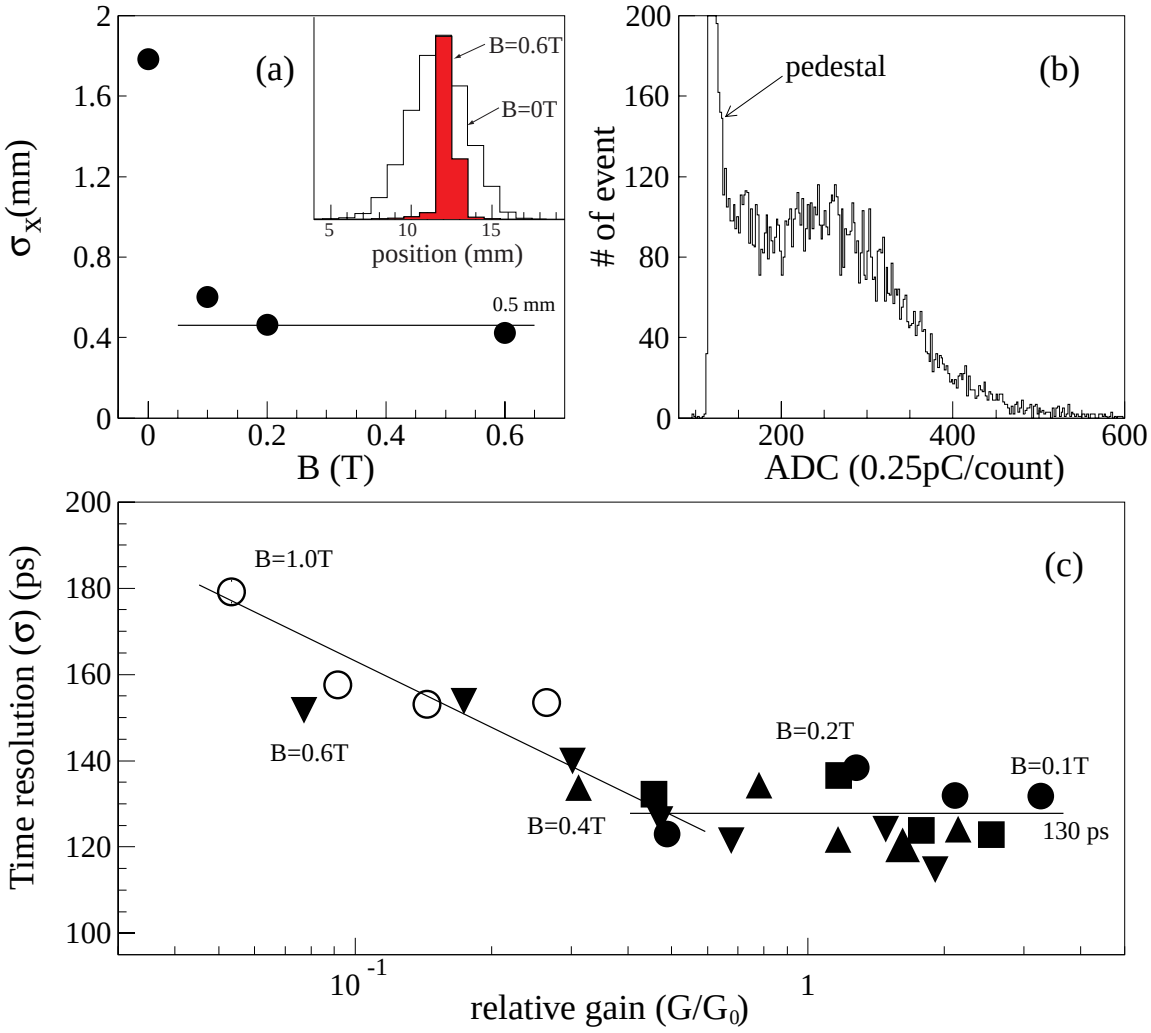

Figure 8: Perfomance of L24 and L24X PMTs. (a) Position resolution (L24) vs magnetic field. Subset is a spartial distributions with and without field. (b) Pulse-height distribution of L24X PMT. (c) Time resolution (σ) of L24X as a function of relative gain (G/G_o), where G_o is the amplification gain with $B = 0$. Individual magnetic field strengths are indicated in the figure. The measurements were carried out using both a light pulser with a single photon emission and a 1 mm-wide slit in front of PMTs.

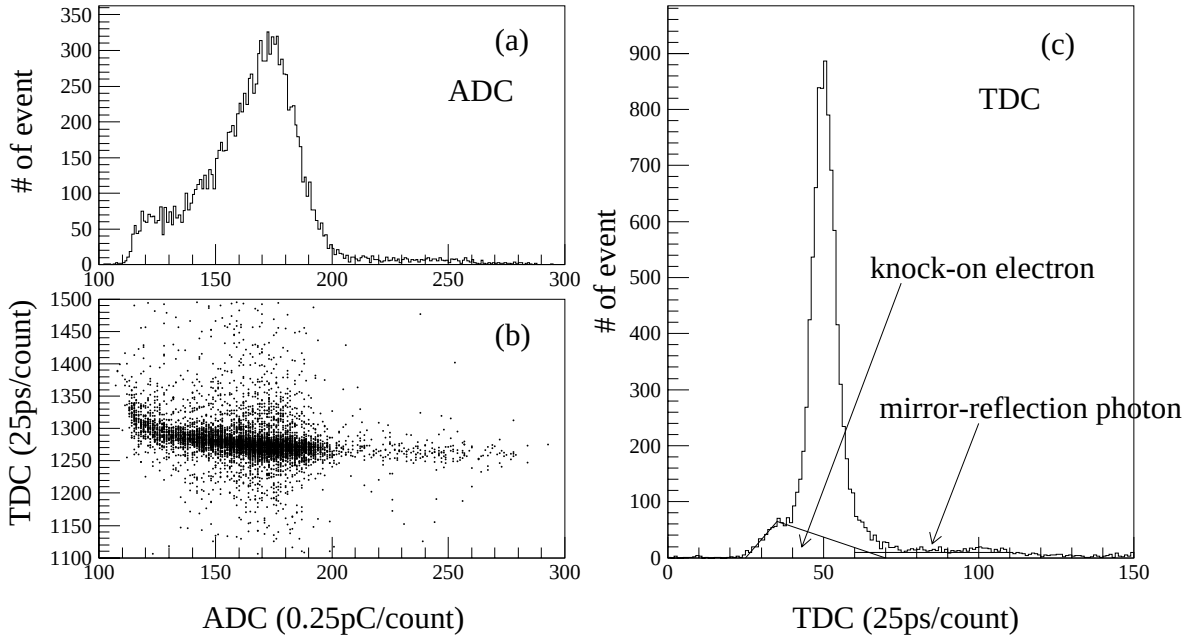

Figure 9: Data obtained in the beam test with L = 0.02 m. (a) ADC distribution, (b) ADC vs TDC scatter plot, and (c) Timewalk corrected TDC distribution. Resolution of σ =80 ps was obtained by subtracting a time uncertainty in the start signal. These data are obtained using the 20th anode, and in a 2 GeV/c π beam.

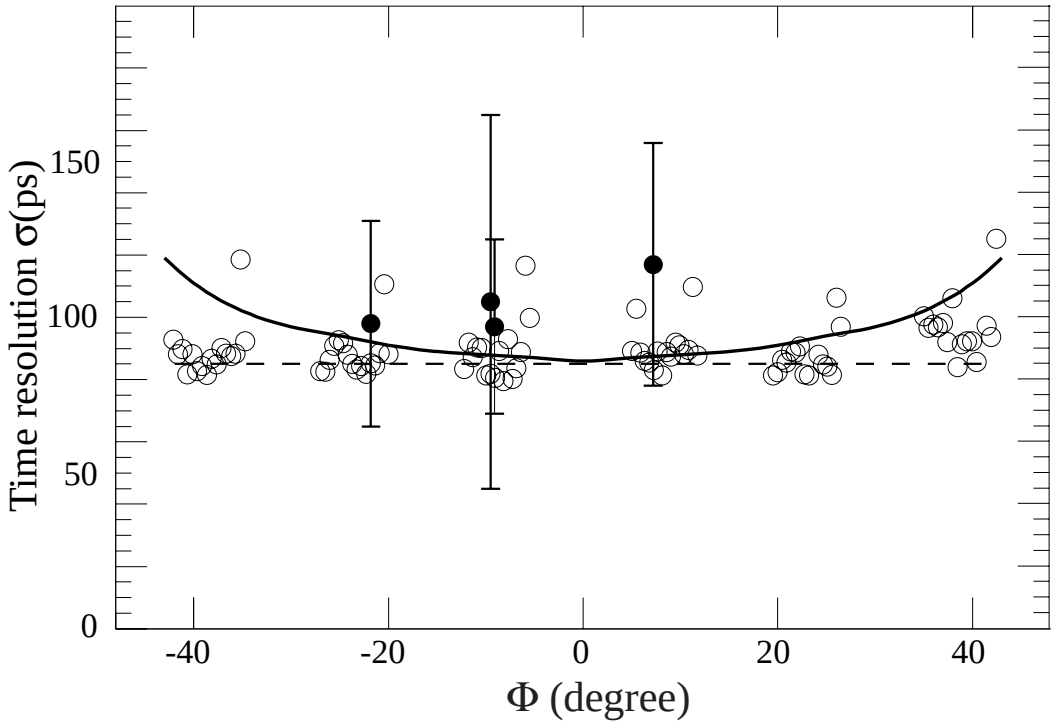

Figure 10: Measured time resolutions over 96 anodes at L = 0.02 m and 1 m for 2 GeV/c πs. Horizontal axis represents the readout anode channels in the form of the Φ angle. Open circles are the measured time resolutions measured at L = 0.02 m, and closed circles with error bars were obtained at L = 1 m by applying a particular analysis method mentioned in the text. The solid curve indicates a MC expectation at L = 1 m, based on the achieved resolution, and at L = 0.02 m, indicated by a dotted line.

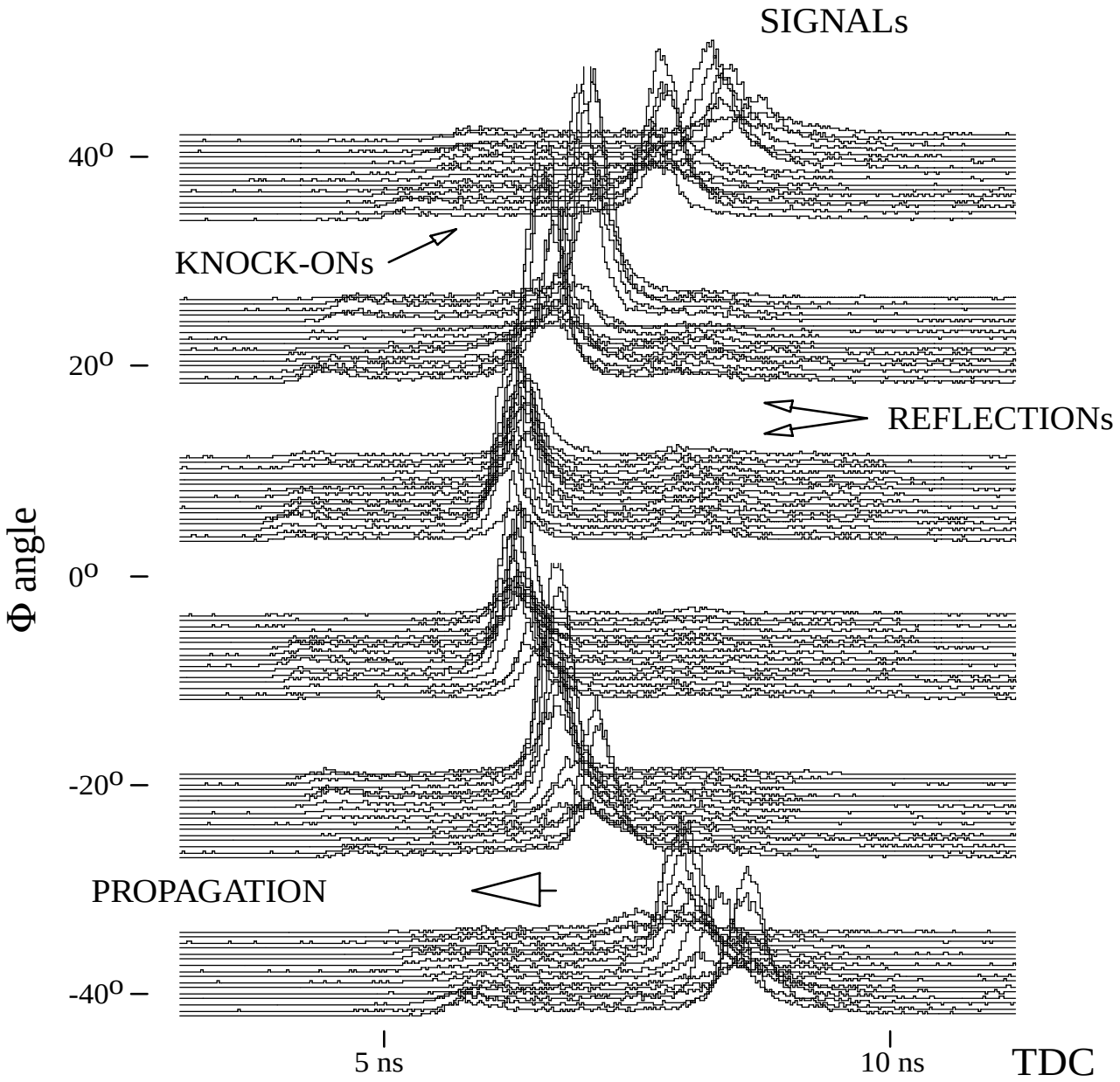

Figure 11: Cherenkov ring image formed by the FW photons, produced by a 4 GeV/c πs beam, perpendicular to the bar, and at L = 1 m. Timewalk is not corrected out.